

Value of low-dose spiral CT combined with circulating miR-200b and miR-200c examinations for lung cancer screening in physical examination population

Y.-Z. WANG¹, Y.-B. LV², G.-Y. LI³, D.-O. ZHANG⁴, Z. GAO⁵, Q.-Z. GAI⁶

¹Department of Clinical Laboratory, Yantaishan Hospital, Yantai, China

²Department of Medical Imaging, Yantai Yuhuangding Hospital, Yantai, China

³Department of Medical Imaging, Laizhou City People's Hospital, Laizhou, China

⁴Public Health Department, The People's Hospital of Zhangqiu Area, Jinan, China

⁵Department of Rehabilitation, The People's Hospital of Zhangqiu Area, Jinan, China

⁶Department of Medical Imaging, Yantaishan Hospital, Yantai, China

Yanzheng Wang and Yongbin Lv contributed equally to this work

Abstract. – OBJECTIVE: The aim of this study is to investigate the clinical value of low-dose spiral CT (LDCT), plasma miR-200b, and miR-200c combined screening for lung cancer screening in the physical examination population.

PATIENTS AND METHODS: From January 2016 to December 2018, the Physical Examination Center of our hospital underwent low-dose spiral CT lung cancer screening for 10,823 people aged ≥ 40 years. The quantitative Real Time-Polymerase Chain Reaction (qRT-PCR) was used to detect the relative expressions of miR-200b and miR-200c in plasma, analyze the imaging characteristics of suspicious nodules in the lung and the relative expressions of miR-200b and miR-200c in plasma.

RESULTS: A total of 2,919 pulmonary nodules were detected in the 10823 physical examination population, with a total detection rate of 26.97%, including 1523 males and 1396 females. 1081 positive nodules were detected with a detection rate of 9.99%. According to the Lung-RADS classification, the number of type 2 nodules was the highest, with a detection rate of 22.13%. Meanwhile, the rate of type 3 nodules was 3.15%, and the rate of type 4 nodules was 1.69%. The sensitivity, accuracy, and negative predictive value of LDCT, miR-200b, and miR-200c in the diagnosis of lung cancer were significantly improved compared with the individual tests, which were 94.74%, 90.16%, and 95.88%, respectively.

CONCLUSIONS: Low-dose spiral CT combined with plasma miR-200b and miR-200c for lung cancer screening in the physical examination population can help to detect lung cancer patients with early symptoms that are not significant, and achieve early diagnosis and early treatment.

Key Words:

Physical examination population, Lung cancer, LDCT, MiR-200b, MiR-200c, Combined screening.

Introduction

Lung cancer is a common malignant tumor. In recent years, the incidence rate has risen, ranking first among all malignant tumors in morbidity and mortality¹. Due to the insidious onset of lung cancer, the early clinical manifestations are not specific, and most patients are already in the advanced stage at the time of consultation, thus losing the best opportunity for surgical treatment. The latest statistics showed that the 5-year survival rate of lung cancer was less than 20%, while the survival rate of surgically resected stage I cancer patients was much higher than 70%². Therefore, early screening for lung cancer is of great significance to reduce the mortality rate. At present, Low-dose CT (LDCT) is a commonly used method for lung cancer screening. LDCT is not only effective in detecting early lung lesions, but also has a lower radiation doses compared with chest X-rays examination, so it is widely used. The National Lung Screening Trial (NLST) in the United States proves that low-dose spiral CT for lung cancer screening can significantly reduce the mortality of lung cancer³. However, there are still some limitations in screening lung cancer by LDCT alone, and there are some misdiagnosis

and missed diagnosis. In recent years, with the in-depth study of molecular biology, it has been found that miRNAs are important factors in various biological processes to regulate the occurrence and development of tumors. Among them, the circulating miRNAs in peripheral blood are free from digestion by RNase and are highly stable in plasma and serum. The convenient detection method of circulating miRNAs in peripheral blood is convenient and has been regarded as a new potential biomarker in cancer screening and early diagnosis, and it is an effective supplement to LDCT examination⁴. This study intends to perform LDCT screening for lung nodules in people aged 40 years or older on physical examination first, and perform plasma miRNA-200b and miRNA-200c tests for suspected nodules. The purpose of this study is to explore the clinical application value of LDCT, plasma miR-200b and miR-200c combined examination in lung cancer screening.

Patients and Methods

Clinical Material

From January 2016 to December 2018, 10,823 medical examiners who were over 40 years old and registered in the medical examination center of our hospital were selected as the research subjects. Lung nodules were screened by LDCT first. Those with suspicious nodules were tested for plasma miR-200b and miR-200c. The International Guidelines for lung cancer diagnosis and screening are according to the National Comprehensive Cancer Network. This investigation was approved by the Ethics Committee of Yantaishan Hospital. Before the study, all participants signed written informed consents.

LDCT Inspection

A SIEMENS SOMATOM (Berlin, Germany) Definition flash spiral CT machine was selected for low-dose lung scanning. For patients with multiple nodules, the dominant lung nodules were selected for analysis. Lung-Reporting and Data System (Lung-RADS) was used to classify lung nodules.

Detection of MiR-200b and MiR-200c in Plasma

The TRIzol RNA extraction reagent was purchased from TaKaRa (Komatsu, Japan). MystiCq[®] miRNA quantitative Real Time-Polymerase Chain Reaction (qRT-PCR) kit and mirPremier[®] miRNA isolation and extraction kit were pur-

chased from Sigma Company (St. Louis, MO, USA). The PCR primers were synthesized by Shanghai Biological Engineering Company (Shanghai, China).

An EDTA (ethylenediaminetetraacetic acid) anticoagulation tube was used to collect 5 mL of venous blood from patients with suspected pulmonary nodules on an empty stomach and mixed, centrifuged at 3000 r/min for 15 min to separate the plasma. The 1.5 mL RNase-free Eppendorf (EP) tubes were used to extract plasma for aliquots and store in a refrigerator at -80°C for inspection.

TRIzol method was used to extract total RNA from serum, and complementary deoxyribose nucleic acid (cDNA) was obtained by reverse transcription using a reverse transcription kit. Quantitative PCR was used to amplify miRNA-200b and miRNA-200c. Reaction system: 0.5 μL each of forward and reverse primers (10 μmol/L), 5.0 μL of polymerase and green fluorescent dye premix, 1.0 μL of cDNA (50 ng/μL), sterile enzyme-free in qRT-PCR kit 3.0 μL of water for a total of 10 μL. The reaction conditions were set as follows: 95°C 90 s, 95°C 30 s, 62°C 30 s, 72°C 20 s, for a total of 40 cycles. After the reaction, U6 was used as an internal reference, and the relative expressions of miRNA-200b and miRNA-200c in different samples were calculated using the $2^{-\Delta\Delta Ct}$ method. qRT-PCR primer sequences are shown in Table I.

Outcome Criteria

If the results of LDCT, miRNA-200b, and miRNA-200c tests are consistent with the pathological diagnosis, it is true positive or true negative, and non-conformity is false positive or false negative. If one or more of the joint inspections are positive, it is considered positive, and all negative is considered negative.

Evaluation Indicators for Diagnostic Tests

Pathological diagnosis is the gold standard. The test results are divided into true positive (a), false positive (b), false negative (c), and true negative (d). The calculation formula are sensitivity = $a / (a + c)$, specificity = $d / (d + b)$, accuracy = $(a + d) / (a + b + c + d)$, and positive predictive value = $a / (a + b)$, negative predictive value = $d / (d + c)$.

Statistical Analysis

The obtained data were analyzed by Statistical Product and Service Solutions (SPSS) 23.0 statistical software (IBM Corp., Armonk, NY, USA). The measurement data is non-normally distributed, expressed as the median. The Wilcoxon rank

Table I. qRT-PCR primer sequences.

miRNA	Sequence
miR-200b	
F	5'-CATTCCGGACTCGAGCACTTGTGA-3'
R	5'-GCTACGTTGAGTCAACTAGTAACG-3'
miR-200c	
F	5'-TGGAGGCCAGTTCACCTCGA-3'
R	5'-ATCTCCAGTGCAGCGGCCTCTG-3'
U6	
F	5'-CTCGCTTCGGCAGCACA-3'
R	5'-AACGCTTACGAATTTGCGT-3'

sum test was used for comparison between the two groups. Count data were expressed as rates (%). The area under the ROC curve (AUC) was obtained according to the receiver operating characteristic (ROC) curve analysis, and the optimal critical values for miR-200b and miR-200c in the diagnosis of lung cancer were obtained according to the Jordan index. The pathological diagnosis was used as the gold standard. The sensitivity, specificity, accuracy, positive predictive value, and negative predictive value of LDCT, miR-200b, and miR-200c in single and combined detection of lung cancer were statistically calculated using the four-table method. $p < 0.05$ was statistically significant.

Result

Comparison of Detection Rates of LDCT pulmonary Nodules Nodule in Different Genders and Age

A total of 2,919 cases of pulmonary nodules were detected by LDCT in 10823 physical examination populations, with a total detection rate of 26.97% (2919/10823). There was no significant difference in the detection rate of pulmonary nodules between male and female groups ($X^2 =$

3.130, $p = 0.077$) ($p > 0.05$). There was a statistically significant difference in the detection rate of lung nodules at different ages ($X^2 = 27.321$, $p = 0.000$) ($p < 0.01$). The highest detection rate of nodules was 50-59 years old, at 29.00% (1393/4804) (Table II).

Comparison of LDCT Imaging Characteristics of Nodules Detected by Different Genders

Pulmonary nodules in 2919 cases were mainly single, solid, and Lung-RADS type 2 nodules. There were no significant differences in the number of nodules, the nature of nodules, and the Lung-RADS classification between the male and female groups ($X^2 = 3.290$, 5.045, 4.084, $p = 0.070$, 0.080, 0.130) (Table III).

Comparison of LDCT Imaging Characteristics of Lung-RADS Type 3 and Type 4 Pulmonary Nodules

Lung-RADS type 4 nodules have irregular shapes, unclear borders, lobular signs, burr signs, pleural depressions, and nodules in the nodules. The incidence of images is significantly higher than that of Lung-RADS type 3 nodules ($p < 0.01$) (Table IV).

LDCT Imaging Characteristics of 183 Cases of Lung-RADS Type 4 Nodules

A total of 183 cases of Lung-RADS 4 nodules were followed up and analyzed by CT imaging. Finally, 78 cases of lung cancer and 105 cases of benign lesions were diagnosed. All 183 cases of Lung-RADS 4 nodules were diagnosed by nodule puncture or postoperative pathological histopathology, 76 cases of lung cancer and 107 cases of benign lesions were diagnosed pathologically. Pathological diagnosis was the gold standard. CT diagnosis of 78 cases of lung cancer was consistent with pathological diagnosis in 66 cases (true positive) and 12 cases were inconsistent (false

Table II. Comparison of lung nodule detection rates in different sexes and age groups.

Groups	n	Nodules [% (n)]	χ^2	p
Gender			3.130	0.077
Male	5798	26.27 (1523/5798)		
Female	5025	27.78 (1396/5052)		
Age (years)			27.321	0.000
40-49	2839	26.95 (765/2839)		
50-59	4804	29.00 (1393/4804)		
60-69	1893	24.93 (472/1893)		
≥ 70	1287	22.46 (289/1287)		

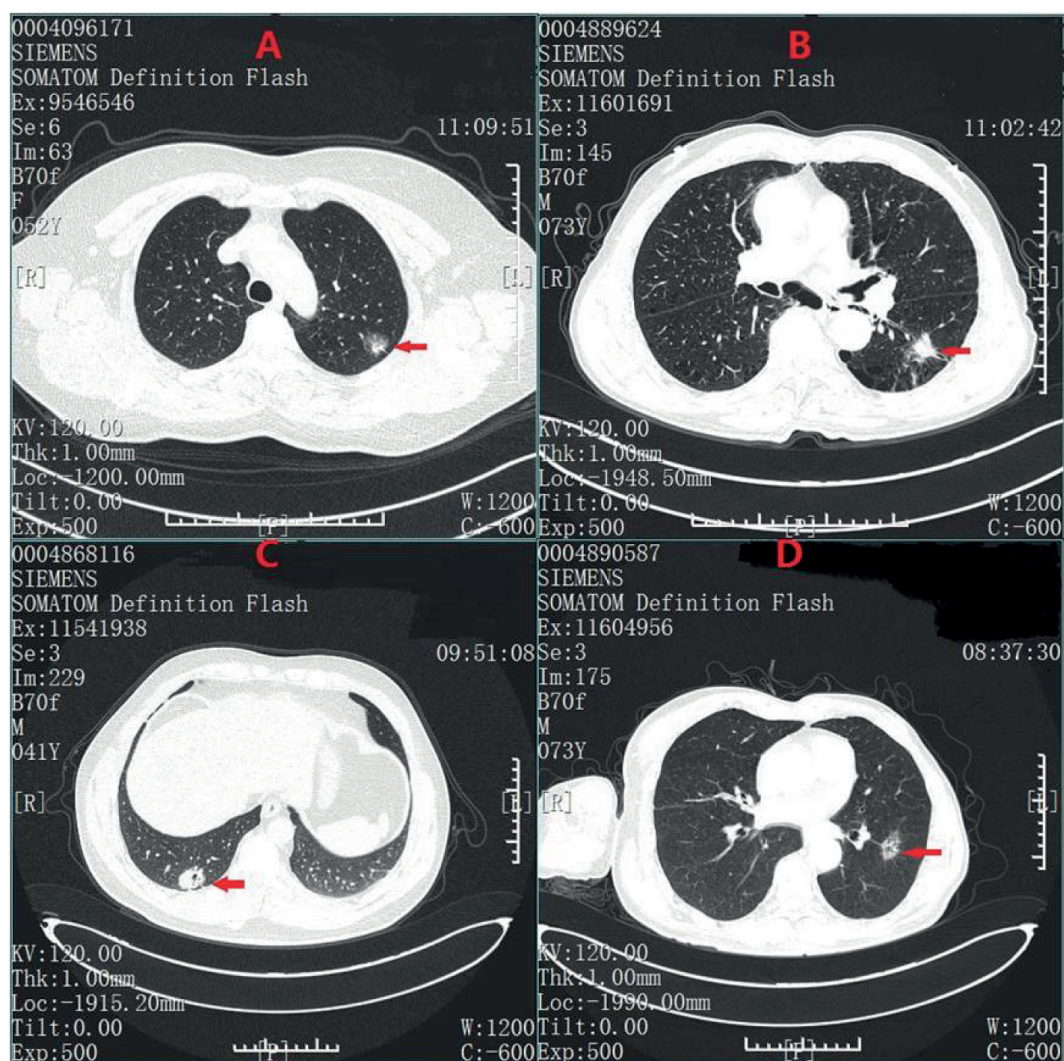


Figure 1. LDCT images of 4 suspected lung nodules confirmed by pathology as lung cancer. **A**, A 52-year-old female. The arrow shows a patch-like mixed ground glass shadow in the subpleural area of the upper lobe of the left lung. The border is unclear. The size is about 13 mm × 14 mm. Postoperative pathological diagnosis: slightly invasive adenocarcinoma. **B**, A 53-year-old man. The arrow shows nodules in the lower lobe of the left lung. The border is unclear. The size is about 20 mm × 16 mm. The leaves are visible. Pathological diagnosis of nodule puncture: invasive adenocarcinoma. **C**, 41-year-old woman. The arrow shows a solid nodule in the lower lobe of the right lung. The edge is blurred. The size is about 20 mm × 18 mm. The leaves are visible. Pathological diagnosis of nodule puncture: adenocarcinoma. **D**, A 63-year-old man with arrows showing irregular nodules in the lower lobe of the left lung, small burrs on the edges, multiple small bubbles inside, a diameter of about 18 mm × 16 mm, and pleural traction near the leaves. Pathological diagnosis of nodule puncture: squamous cell carcinoma (medium differentiation).

positives). CT diagnosis of 105 benign lesions was consistent with pathological diagnosis in 95 cases (negative) and inconsistent in 10 cases (false negative). LDCT images of 76 cases of lung cancer showed irregular shapes in 44 cases and unclear nodular boundaries in 45 cases. Forty-seven nodules showed lobular signs, 42 nodules showed glitch signs, 38 nodules showed pleural depression signs, and 42 nodules had vascular penetration. The lung cancer LDCT image is shown in Figure 1.

Comparison of the Relative Expression of MiR-200b and MiR-200c in Peripheral Blood of Patients with Lung Cancer and Benign Pulmonary Lesions

The relative expression levels of plasma miR-200b and miR-200c in 183 patients with Lung-RADS type 4 (suspected malignant) nodules were measured. The pathological diagnosis was the gold standard and they were divided into lung cancer group (76 cases) and benign lesion group (107 cases). The areas under the ROC curve (AUC) for miR-

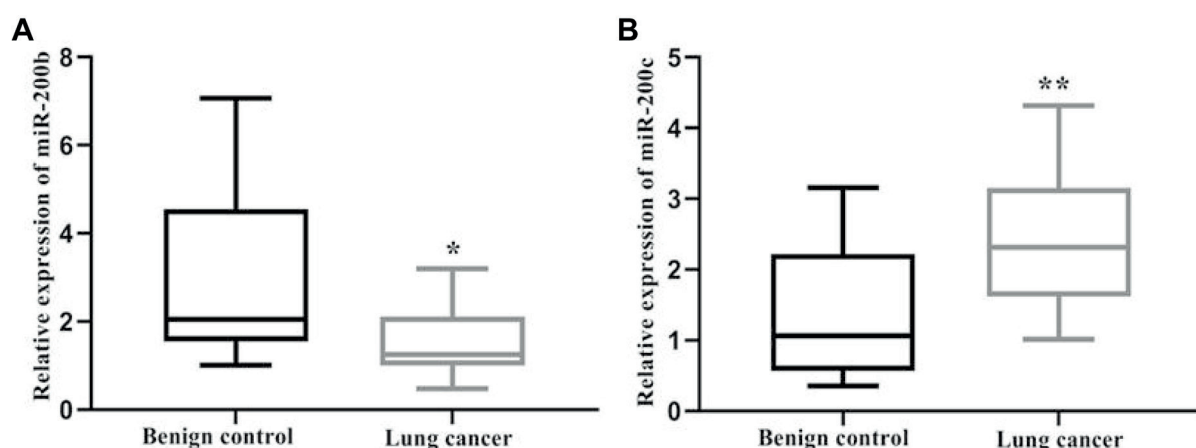


Figure 2. Comparison of relative expression levels of plasma miRNA (miR-200b and 200c) in lung cancer group and benign lung disease group. **A**, The relative expression of miR-200b in lung cancer plasma was significantly lower than that in the benign lesion group. **B**, The relative expression of miR-200c in lung cancer plasma is significantly higher than that in the benign lesion group. * $p < 0.05$, ** $p < 0.01$.

200b and miR-200c in the diagnosis of lung cancer were 0.698 and 0.769, respectively, and the approximate indices were 0.526 and 0.579, respectively. The optimal cut-off values for lung cancer diagnosis were 1.57 and 2.07. The results showed that the relative expression of plasma miR-200b in patients with lung cancer was significantly lower than that in benign lesions ($U = 94.000$, $p = 0.012$), while the relative expression of plasma miR-200c in patients with lung cancer was significantly higher than that in benign lesions ($U = 83.500$, $p = 0.005$) (Figure 2).

Comparison of the value of LDCT, MiR-200b, MiR-200c Single and Combined Screening for Lung Cancer

The results of LDCT, miR-200b, miR-200c and the combined examination were compared with

pathological diagnosis (Table V). The sensitivity, accuracy, and negative predictive value of LDCT, miR-200b, and miR-200c in the screening of lung cancer were significantly improved compared with individual tests ($p < 0.05$) (Table VI).

Discussion

Studies have shown that lung nodules are closely related to the occurrence of lung cancer. Based on the imaging characteristics of lung positive nodules and related risk factors, a lung cancer risk prediction model can be constructed to predict the probability of lung cancer⁵. In recent years, low-dose spiral CT has been widely used for lung cancer screening in asymptomatic peo-

Table III. Comparison of LDCT imaging characteristics of nodules detected by different genders.

Imaging features	Male [% (n)]	Female [% (n)]	χ^2	P
Numbers			3.290	0.070
Single	55.29 (842/1523)	51.93 (725/1396)		
Multiple	44.71 (681/1523)	48.07 (671/1396)		
Nodules type			5.045	0.080
Solid	84.96 (1294/1523)	82.09 (1146/1396)		
Partial solidity	4.01 (61/1523)	5.37 (75/1396)		
Ground glass	11.03 (168/1523)	12.54 (175/1396)		
Lung-RADS classification			4.084	0.130
Type 2	82.14 (1251/1523)	81.95 (1144/1396)		
Type 3	12.34 (188/1523)	10.96 (153/1396)		
Type 4	5.52 (84/1523)	7.09 (99/1396)		

Table IV. Comparison of LDCT imaging characteristics of Lung-RADS type 3 and type 4 pulmonary nodules.

Imaging features	Lung-RADS type 3 [% (n)]	Lung-RADS type 4 [% (n)]	χ^2	<i>P</i>
Shape			240.788	0.000
Rule	96.77 (330/341)	35.52 (65/183)		
Irregular	3.23 (11/341)	64.48 (118/183)		
Boundary			93.951	0.000
Clear	91.79 (313/341)	55.74 (102/183)		
Unclear	8.21 (28/341)	44.26 (81/183)		
Internal structure				
Foliage sign	1.17 (4/341)	26.76 (49/183)	85.866	0.000
Glitch sign	1.76 (6/341)	15.85 (45/183)	70.655	0.000
Pleural depression	0.59 (2/341)	13.66 (40/183)	73.086	0.000
Vascular penetration	6.74 (23/341)	28.42 (45/183)	33.909	0.000

ple. The principle of LDCT is based on the histological characteristics of lung tissues and other organ structures, and it uses the characteristics of high lung air content and low density. LDCT only requires a lower dose of radiation to form a more satisfactory image. The thin-layer scanning and reconstruction technology of LDCT can clearly display the cross-sectional image and perform 3D reconstruction observation. It can be seen that the ground glass density, lobulation sign, glitch sign, pleural depression, nodules in blood vessels in the nodule and other signs, and is of great significance for early diagnosis of lung cancer⁶. LDCT maintains the sensitivity of conventional CT, and the imaging radiation dose is lower. Compared with ordinary chest X-rays, LDCT can detect more lung nodules and early lung cancer. The New York Early Lung Cancer Initiative conducted an LDCT examination of 6,295 cases of asymptomatic smokers over 60 years of age. 101 cases of lung cancer were detected, 91.30% had no definite clinical metastases, of which 20 cases were found during the later follow-up, 85% patients were still

in the early stage and have not occurred metastasis. It fully demonstrates that LDCT can screen a higher proportion of early lung cancer⁷. The results of this study showed that the pulmonary nodule detection rate of LDCT scans of 10823 people aged ≥ 40 years was 26.97% (2919/10823), which was similar to the screening test of Horeweg et al⁸. The detection rate of lung positive nodules was 9.99% (1081/10823), which was lower than the 16.00% reported by Henschke et al⁹. 76 cases of lung cancer were diagnosed by pathology, and the detection rate of lung cancer was 0.70% (76/10823), which was lower than 1.50% of Yang et al¹⁰, and close to 0.80% of Pastorino et al¹¹. This study showed that the detection rate of nodule in the 50-59 age group is the highest (29.00%), and lung cancer screening should be strengthened in this age group in the future. The results of this study also showed that the sensitivity and specificity of LDCT for lung cancer screening were 86.84% and 88.79%. There are certain false positives and false negatives, and there may be some misdiagnosis and missed diagnosis. Therefore, it

Table V. LDCT, miR-200b, miR-200c test results compared with pathological diagnosis.

Project		Pathological diagnosis	
		Positive (n)	Negative (n)
CT	Positive (n)	66	12
	Negative (n)	10	95
miR-200b	Positive (n)	53	6
	Negative (n)	23	101
miR-200c	Positive (n)	51	5
	Negative (n)	25	102
Joint inspection	Positive (n)	72	14
	Negative (n)	4	93

Table VI. Comparison of the value of LDCT, miR-200b, miR-200c single and combined screening for lung cancer.

Detection Indicator	Sensitivity	Specificity	Accuracy	Positive predictive value	Negative predictive value
CT	86.84 (66/76)	88.79 (95/107)	87.98 (161/183)	84.62 (66/78)	90.48 (95/105)
miR-200b	67.11 (51/76)	95.33 (102/107)	83.61 (153/183)	91.07 (51/56)	80.31 (102/127)
miR-200c	69.74 (53/76)	94.39 (101/107)	84.15 (154/183)	89.83 (53/59)	81.45 (101/124)
Combination detect	94.74 (72/76) *	86.92 (93/107)	90.16 (165/183) *	83.72 (72/86)	95.88 (93/97) *
χ^2	25.040	6.952	10.417	2.391	15.398
<i>p</i>	0.000	0.073	0.015	0.795	0.002

**p*<0.05.

is recommended that LDCT combine with other methods to screen for suspicious nodules.

MiRNA disorders are closely related to the occurrence and development of lung cancer. MiRNAs regulate cancer cell proliferation, apoptosis, metastasis, invasion and cell cycle through some pathways or genes, and exhibits carcinogenic or suppressive properties. The application of miRNA in tumor diagnosis, treatment and prognosis provides potential research value. MiRNAs in the peripheral blood circulation are not easily degraded by RNases. The stability of blood miRNA and the convenience of detection make it a new biological indicator for cancer diagnosis¹². MiR-200b and miR-200c are members of the miRNA-200 family. In recent years, many studies have shown that miR-200b and miR-200c are involved in tumorigenesis, development, metastasis, and drug resistance¹³.

It has been reported that the expression of miR-200c is significantly increased in colon cancer tissues, and miR-200c may play a carcinogenic role. In this study, the relative expression levels of miR-200b and miR-200c were analyzed in the plasma of 76 cases of lung cancer and 107 cases of benign lung lesions. The results showed that the relative expression of miR-200b in the lung cancer group was significantly lower than that in the benign lesion group, while the relative expression of miR-200c in the lung cancer group was higher than that of the control group. The sensitivity of miR-200b and miR-200c in diagnosing lung cancer was 67.11%, 69.74%, respectively. Therefore, plasma miR-200b and miR-200c can be used as biological indicators for early diagnosis of lung cancer, and can provide important supplements for LDCT screening, but the sensitivity is still not satisfactory. The novelties of this study is that we use low-dose spiral CT combined with plasma miR-200b and miR-200c to detect lung cancer for the first time.

Conclusions

Low-dose spiral CT combined with plasma miR-200b and miR-200c can be used to screen lung cancer for people undergoing physical examination, which is helpful for early diagnosis of lung cancer. In the future, the follow-up time for positive nodules should be extended to prevent early diagnosis of lung cancer.

Conflicts of interest

The authors declare that they have no conflicts of interest.

References

- 1) Bray F, Ferlay J, Soerjomataram I, Siegel RL, Torre LA, Jemal A. Global cancer statistics 2018: GLOBOCAN estimates of incidence and mortality worldwide for 36 cancers in 185 countries. *CA Cancer J Clin* 2018; 68: 394-424.
- 2) Liang W, Shao W, Jiang G, Wang Q, Liu L, Liu D, Wang Z, Zhu Z, He J. Chinese multi-institutional registry (CMIR) for resected non-small cell lung cancer: survival analysis of 5,853 cases. *J Thorac Dis* 2013; 5: 726-729.
- 3) Aberle DR, Adams AM, Berg CD, Black WC, Clapp JD, Fagerstrom RM, Gareen IF, Gatsonis C, Marcus PM, Sicks JD. Reduced lung-cancer mortality with low-dose computed tomographic screening. *N Engl J Med* 2011; 365: 395-409.
- 4) Heegaard NH, Schetter AJ, Welsh JA, Yoneda M, Bowman ED, Harris CC. Circulating micro-RNA expression profiles in early stage nonsmall cell lung cancer. *Int J Cancer* 2012; 130: 1378-1386.
- 5) Katki HA, Kovalchik SA, Petito LC, Cheung LC, Jacobs E, Jemal A, Berg CD, Chaturvedi AK. Implications of nine risk prediction models for selecting ever-smokers for computed tomography lung cancer screening. *Ann Intern Med* 2018; 169: 10-19.
- 6) Kim TJ, Goo JM, Lee KW, Park CM, Lee HJ. Clinical, pathological and thin-section CT features of persistent multiple ground-glass opacity nodules:

- comparison with solitary ground-glass opacity nodule. *Lung Cancer* 2009; 64: 171-178.
- 7) New York Early Lung Cancer Action Project Investigators. CT Screening for lung cancer: diagnoses resulting from the New York Early Lung Cancer Action Project. *Radiology* 2007; 243: 239-249.
 - 8) Horeweg N, Nackaerts K, Oudkerk M, de Koning HJ. Low-dose computed tomography screening for lung cancer: results of the first screening round. *J Comp Eff Res* 2013; 2: 433-436.
 - 9) Henschke CI, Yip R, Yankelevitz DF, Smith JP. Definition of a positive test result in computed tomography screening for lung cancer: a cohort study. *Ann Intern Med* 2013; 158: 246-252.
 - 10) Yang W, Qian F, Teng J, Wang H, Manegold C, Pilz LR, Voigt W, Zhang Y, Ye J, Chen Q, Han B. Community-based lung cancer screening with low-dose CT in China: results of the baseline screening. *Lung Cancer* 2018; 117: 20-26.
 - 11) Pastorino U, Rossi M, Rosato V, Marchiano A, Sverzellati N, Morosi C, Fabbri A, Galeone C, Negri E, Sozzi G, Pelosi G, La Vecchia C. Annual or biennial CT screening versus observation in heavy smokers: 5-year results of the MILD trial. *Eur J Cancer Prev* 2012; 21: 308-315.
 - 12) Ferracin M, Veronese A, Negrini M. Micromarkers: miRNAs in cancer diagnosis and prognosis. *Expert Rev Mol Diagn* 2010; 10: 297-308.
 - 13) Humphries B, Yang C. The microRNA-200 family: small molecules with novel roles in cancer development, progression and therapy. *Oncotarget* 2015; 6: 6472-6498.